

1
2
3
4
5
6
7
8
9
10
11
12
13
14
15
16
17
18
19
20
21
22
23
24
25
26
27
28
29
30
31
32
33
34
35
36
37
38
39
40
41
42
43
44
45
46
47
48
49
50
51
52
53
54
55
56
57
58
59
60
61
62
63
64
65

An Artificial Neural Network for fuel efficiency analysis for cargo vessel operation

Mei Ling Fam*, Zhi Yung Tay, Dimitrios Konovessis

Singapore Institute of Technology, SIT@Dover, 10 Dover Drive Singapore 138683

Abstract

There is increasing interest in understanding fuel consumption from the perspective of increasing energy efficiency on a vessel. Thus the aim of this paper is to present a new framework for data-driven estimation of fuel consumption by employing a combination of (i) traditional statistical analysis and (ii) Artificial Neural Networks. The output of the analysis is the most frequently occurring fuel-speed curves corresponding to the respective operational profile. The inputs to the model consider important explanatory variables like draft, sea current and wind. The methodology is applied to a case study of a fleet of 9000 twenty-foot equivalent units (TEU) vessels, in which telemetry data on the fuel consumption, vessel speed, current, wind direction and strength were analysed. The performance of the method is validated in terms of error estimation criterion like R^2 values and against physical phenomena obtained from the data. The results can be used to study the economic and environmental benefits of slow-steaming and or fuel levies, or by extending this part of the model into exergy analysis for a more holistic review of energy saving initiatives.

Keywords: Fuel consumption in vessels, Artificial neural networks, telemetry data

1. Introduction

1.1. Aim of study

Fuel efficiency of ships have, in recent years, been of interest due to the volatility of fuel prices and environmental considerations. The volatility of

*Corresponding author

Email address: Meiling.Fam@SingaporeTech.edu.sg (Mei Ling Fam)

1
2
3
4
5
6
7
8
9
10 the fuel prices, especially when it is high, have become significant economic
11 driving forces to optimise each voyage, as fuel costs can exceed 50% of a
12 carrier's cost when sailing speeds and fuel costs are high [1],[2].

13 In terms of environmental concerns, the International Maritime Organi-
14 sation (IMO) set up a goal of 50% reduction of GHG emission by 2050 [3] in
15 order to reduce the footprint of ships significantly. As of 1 Jan 2019, ships
16 greater than 5000 tonnes are required to have continuous monitoring on fuel
17 consumption [3]. This legal requirement drives pushes for improved emis-
18 sions control via a holistic approach with access to real-time information on
19 fuel consumption.

20
21 The paper proposes to process telemetry data in a data-driven model
22 to predict the fuel-speed curves under varying operational profiles. The
23 operational profiles in turn are largely segmented by port-to-port journeys
24 as the effect of current and wind are geographically determined and thus
25 confined to vessel journey segments, while the average draft is generally
26 fixed from one port to the next.
27
28

29 *1.2. Literature review*

30
31 Fuel consumption of a ship is of interest as an important piece of infor-
32 mation for several decision-making points on its operation profiles. It has a
33 direct impact on the journey cost, and emission goals.

34 The ship's power vs speed curve that is prepared during the delivery sea
35 trials are usually the first point of reference, but these are usually based on
36 a limited range of sea-states, thus this is not representative of the sea-faring
37 scenario most of the time.
38

39 The prediction of fuel-speed functions can be classified in three ways (i)
40 data-based (ii) naval architecture principles (iii) hybrid of methods (i) and
41 (ii). In recent years, methods steer towards methods (i) and (iii), either as a
42 full data-based or a combination of naval architecture principles and data-
43 based methods. This is largely due to numerical or theoretical methods
44 which are complicated to replicate the results measured under operation
45 conditions. The goal of this paper is also to use telemetry data present
46 onboard a vessel to estimate its fuel consumption, thus the literature review
47 is focussed on either data-based or a combination of data-based and naval
48 architecture principle models.
49
50

51 There are several documented methods to estimate fuel consumption
52 from statistical methods such as Bialystocki et al's [4]paper on considering
53 inputs on draft and sea-state and its effect on fuel consumption. However,
54 the fuel consumption output is a multiple step filtering of separate fuel-speed
55 curves. This method, while it bridges the gap of insufficient data, may not
56
57
58

1
2
3
4
5
6
7
8
9
10 accurately consider the combined effect of wind strength and wind direction
11 on fuel consumed. However, the classification of the data preparation into
12 the statistical model is robust and referred in this paper. Other researchers
13 such as Adland et al [5], Magirou et al [6], Yao et al [7], Wang et al [8],
14 Meng et al [9], Ng et al [10] and Lindstad et al [11] consider a number of
15 factors that may affect the residual resistance, such as hull condition, water
16 depth, water temperature, wave etc. However, speed is considered as the
17 main factor in determining fuel consumption. These methods only consider
18 fuel-speed consumption on a constant elasticity for a vessel's port-to-port
19 journey.
20

21 Researchers like Leifsson et al [12] and Coraddu et al [13] combine ele-
22 ments of modelling methods (i) and (iii) which involves naval architecture
23 principles and data-driven models (called 'grey-box models'). In their analy-
24 sis, the grey-box and black-box models performed better than the white-box
25 models. However, the short-comings of using a grey or black box model of
26 not be able to extrapolate information from data gaps is highlighted in the
27 paper. Other researchers such as Abdel Naby et al [14] have used Artificial
28 Neural Networks (ANN) to predict specific residual resistance of a vessel in
29 shallow water, for which design parameters can be improved for the next
30 iteration of vessel design.
31

32
33 Regardless of the methods used to derive fuel-speed curves, Adland et al
34 [5], in particular, highlights that the assumption of constant fuel-speed con-
35 sumption elasticity needs to be re-evaluated. Wang et al [15] also reported
36 that the coefficient of fuel-speed curves of container ships varies from 2.7 to
37 3.3. Tsitsilonis et al [16] also proposed a method to capture propeller curves
38 under different operational profiles.
39

40 Tsitsilonis et al [16] proposed to use Kernel Density Estimates (KDE)
41 to identify shaft power as a function of the density bins the data belongs to.
42 Each shaft power data bin, together with the respective vessel speed forms
43 an operational profile. The most frequently occurring profile is the highest
44 peak demonstrated on the KDE plot. However the method, applied on cargo
45 vessels, bulk carriers and Very Large Crude Carriers (VLCCs), only yielded
46 differentiating power-speed curves for VLCCs which travel on ballast and
47 laden journeys. The power-speed curves for container ships and bulk carriers
48 only had one such curve after the analysis, which does not reflect general
49 conditions.
50

51 Thus, in order to work around the lack of data and in differentiating
52 a wider variety of operational profiles, the method proposed in this paper
53 aims to combine data categorisation from Bialystocki et al [4] and simplifica-
54 tion of the KDE method to group fuel-speed data groups and the addition of
55
56
57

an ANN to identify operating profiles not discerned in the methods described above. This paper attempts to highlight the variances in the fuel-speed data and draw relationships between the variances in the ship resistance, by using an analytical and systematic method to come up with more accurate, updated fuel-speed curves according to the operational profile.

This article is divided into several parts. In Section 2, the statistical treatment of data is introduced. Section 3 discusses the theory and set-up of the ANN. It also identifies how the parameters affect fuel consumption estimation. The results from several case studies are presented in Section 4 including a discussion of results. Section 5 discusses the application of the model. The conclusions of this study are presented in Section 6.

2. Methods and data

2.1. Modelling of ship fuel consumption

The data used in the model is obtained from the telemetry system on board a fleet of two sister vessels of 9000 twenty-foot equivalent units (TEU) capacity. The main characteristics of the analysed ship are listed in the table below (Table 1):

Table 1: Main characteristics of fleet of ship.

Type	9000 TEU container ship
Built	2013
Length LOA (m)	328.2
Width (m)	45.2
Moulded depth (m)	27.1
Summer Draft (m)	14.5
Deadweight (ton)	108,600
Shaft Power at Maximum continuous rating (MCR) (kw)	51,070

Fuel consumption of a vessel is linked to the resistance that a ship encounters. A theoretical discussion on the contribution of all parameters can be identified in Stopford [1] and Andersen et al [17]. Bialystocki et al [4] highlighted three parameters in their statistical analysis of fuel consumption as : (i) increased draft and displacement (ii) worsening of weather conditions and (iii) worsening of hull and propeller roughness.

For this analysis, there is no access to hull condition. Thus the five factors that could relate to item (i) and (ii) and are accessible as telemetry data, are identified below:

- Vessel speed
- Average draft
- Current
- Wind direction and wind speed
- Vessel journey: High seas vs sheltered water

First and foremost, vessel speed has a major impact on fuel consumption. This relationship is characterised by a power function, suggesting that a higher speeds, there is a non-linear increase in fuel consumption if other conditions remain constant.

Average draft is used as an indication of the intended cargo weight and arrangement in the cargo holds.

The sea-state can be used to classify the subsequent three parameters.

Current can act as an aid or impediment to a vessel depending on the direction of current and the vessel's travelling direction. If current is against the vessel, the vessel experiences greater resistance. Current has both vector and scalar qualities. However as no separate sensor is available, the current can only be estimated from the ship's speed over ground and the ship's speed through the water, taking into account the course, heading and wind influence on the ship. The scalar quantity of current is recorded as knots (kn) based on telemetry data on the difference between the water speed and vessel speed-over-ground.

The weather a ship faces during voyage has significant influence on her fuel consumption, in particular relating to prevailing wind and waves. Normally, a 10 - 15% weather margin [18] is taken into account in design calculations. Head wind requires more power for the ship to advance; therefore more fuel is consumed by the main engine. A tail wind, on the other hand, decreases the amount of fuel consumed. Depending on the cargo load, a beam wind can also have significant influence on the fuel consumption. The forces of the wind are classified according to Beaufort scale, while the wind direction is based on relative angle range from 0 - 180 degrees, which are then filtered into 3 categories : Head (0 - 60 degrees), Beam (60-120 degrees), Tail wind (120-180 degrees). The method on classifying wind speed and direction is based on Bialystocki et al's [4] method.

Vessel leg is used to confine random effects to a journey leg, as the cargo load does not change during the journey from Port A to Port B, and also the local weather or journey conditions can have a significant effect on the ANN modelling accuracy.

Operational data from two sister ships are collated and used as part of the modelling. In general, this is done to work around the issue of data scarcity from confidential commercial operations. The data from both ships are compared and it is noted that due to the same routing and similar cargo load (i.e. operational profiles) the variance between the data is of an acceptable range. In terms of how reliable the data obtained from the system installed on the ship is, in general, there is a physical agreement between the variation in fuel consumed with respect to the environmental conditions and the cargo load. In Section 5 Validation and Benchmarking, Figure 7 highlights the variation in fuel consumed with respect to the channel conditions of current and wind acting against the vessel.

2.2. Data treatment

The first part of data analytics involves the use of the appropriate data for the analysis. This refers to cleaning the data of erroneous values, for e.g. sensors cannot cover every operational profile and may register negative values which do not make sense in the physical world. Data is also categorised according to vessel journey as literature [16]. In a typical vessel journey, the cargo load is expected to remain the same in the leg of the journey. The decision behind the vessel speed would be dependent on the schedule to meet at the upcoming port or the weather conditions. Segmenting the data into vessel journey would reflect the clustering of data, roughly according to the decision-making time frame along a payload journey and, the local-regional weather condition.

The data entries corresponding to the engine steady state operation are identified.

1. The engine power versus speed data set is split into individual data sets corresponding to each vessel voyage. One voyage is defined as the travel from the origin to the destination port (i.e. the one leg of a round voyage).
2. The fuel consumption data (in tonnes/day) from each voyage is then expressed as a Kernel Density Function (KDF) in order to identify the most frequently occurring operational profile. Each local maximum is classified as an vessel operational profile.
3. The specific kernel probability distributions of the fuel consumption bins (from 1 minima to the next minima) are extracted together with the corresponding parameters.
4. Using the categorised engine power data, an ANN model is trained according to the current direction and strength, wind direction and

strength, average draft of vessel and speed of vessel. The output of the model is the fuel consumption[t/d].

5. Upon a satisfactory learning of the ANN, simulation is carried out according the desired operational profile to predict the fuel consumed.

2.3. Kernel density estimation

The use of a Kernel Density Estimate (KDE) is a non-parametric way to estimate the probability density of a random variable. The random variable of interest is the fuel consumption of the vessel in [t/d]. A plot of the fuel probability density functions demonstrates that parametrised models (such a Gaussian distribution) would not accurately describe the multi-modal fuel data. KDEs are closely related to histograms. The use of a suitable kernel can mimic the smoothness or continuity of the probability distribution of fuel data. (see Figure 1). One benefit of using this method is the ability to separate the data into bins which reflect different operation decisions or conditions of travel.

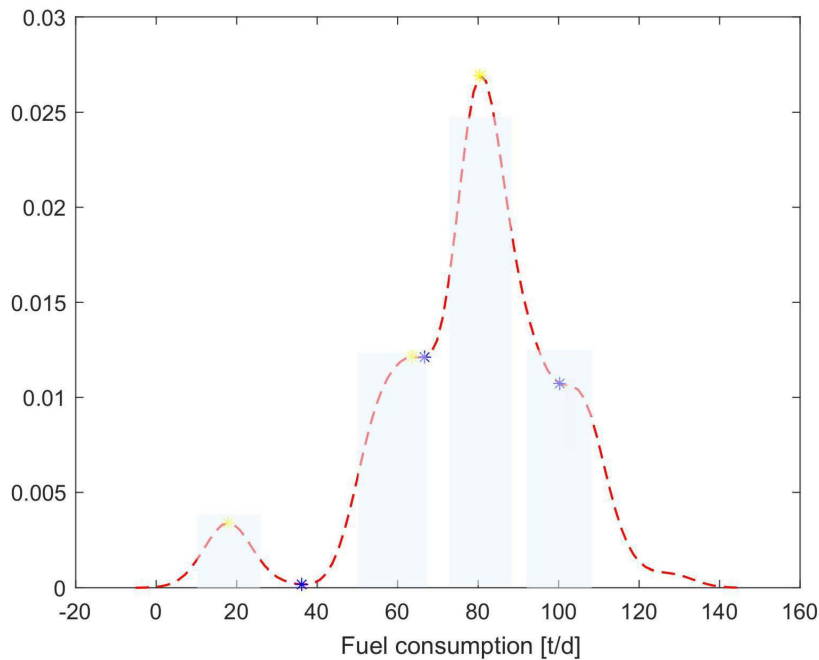


Figure 1: A KDE constructed using the data of fuel consumption [t/d] for a vessel journey, usually defined as a Port A to Port B journey.

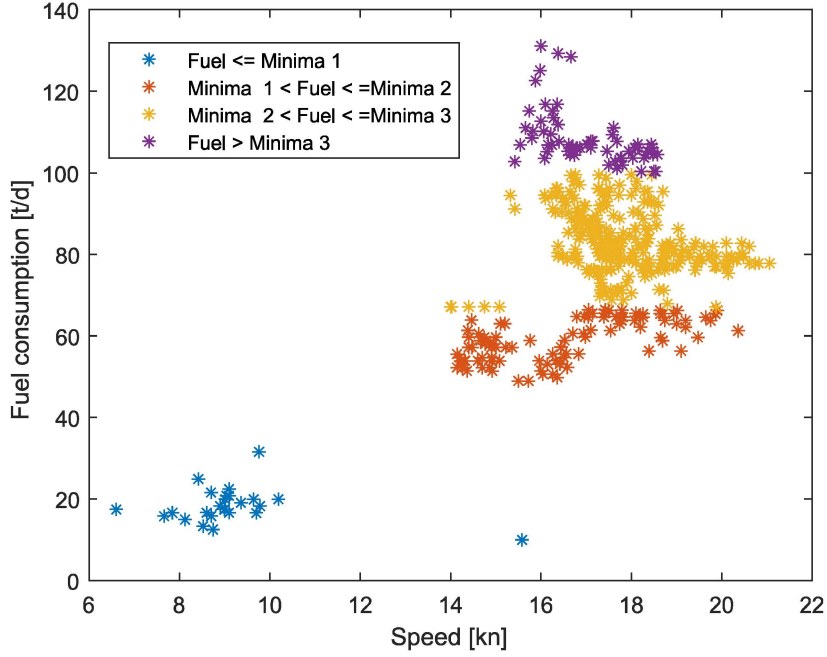


Figure 2: Fuel-speed plot as clustered and colour coded according to the KDE of fuel consumption for vessel journey between two ports.

The shape of the function is estimated through a kernel density estimator $\hat{f}_h(x)$:

$$\hat{f}_h(x) = \frac{1}{n} \sum_{i=1}^n \delta(x - x_i) = \frac{1}{nh} \sum_{i=1}^n K\left(\frac{x - x_i}{h}\right) \quad (1)$$

where (x_1, x_2, \dots, x_n) are independent fuel consumption samples drawn from a distribution with an unknown density f at any given point x . K is the kernel and h is a smoothing parameter called the bandwidth. K_h is the scaled kernel and defined as $K_h(x) = 1/h \cdot K(x/h)$. Both K and h are non-negative functions. The selection of the bandwidth, h , has to be optimal in the trade-off between an overly smooth or overly noisy function. An overly-smoothed function does not yield extra information. An overly noisy distribution with too many extrema is inconclusive. With reference to the optimisation of bandwidth, the Silvermans reference bandwidth is used [16]. The Silvermans reference bandwidth h_I is defined as:

$$h_I = 0.9[\min(\frac{IQR(x)}{1.34}, \sigma)] \cdot n^{(-1/5)} \quad (2)$$

where IQR is the interquartile range of the random variable, fuel consumption, x and σ the standard deviation of the sample. This is a rule-of-thumb estimator where the underlying goal is to select a bandwidth that minimises the mean integrated squared error. With a determined bandwidth, the fuel consumption data is filtered into bins k_x from the KDE:

$$k_x = \operatorname{argmax}(f_{h_I}(x)) \quad (3)$$

where the most frequently occurring values corresponding to the local maxima is determined and sorted into operational profile I of the voyage.

3. Design and performance of the ANN model

In general, an ANN consists of three segments, an input layer, an output layer and a hidden layer (see Figure 3). In the input layer, each neuron receives inputs $a_{j=1}, a_{j=2}, \dots, a_{j=n}$ attached with a weight a_j which indicates the connection strength for a particular input for each connection. Then it multiplies every input by the corresponding weight of the neuron connection. At the input layer, there is also a bias neuron $b1_i$, which can be described as a type of connection weight with a constant non-zero value added to the summation of inputs and corresponding weights. In the hidden layer between input and output layer, activation functions create the output. The activation functions can be stepwise to reflect binary outputs or sigmoid to produce a range of values. Generally there could be more than one hidden layer. The number of hidden layers and the number of neurons in each hidden layer need to be identified and are usually optimised by trial and error; the initial weights are randomised to start the training process. During the different trials, the data was divided into three different subsets: training, cross validation and testing. Cross validation set is used as a signal to stop the training and prevent over training. The determination coefficient is used for measuring ANNs performance.

Fuel consumption of the ship is measured in tonnes/day and is the output of interest in the ANN model. The inputs to the ANN model are current, wind strength, wind direction, vessel speed and average draft. The inputs are refined according to literature review such as that of Bialystocki et al [4]. The following equations which demonstrate the mechanism of a neuron are described below and with respect to Figures 4 - 5.

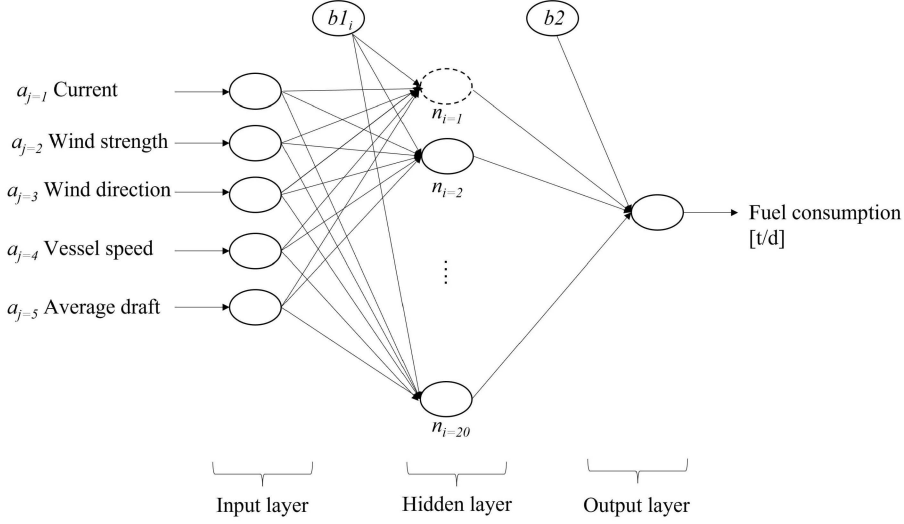


Figure 3: General structure of an ANN with five inputs and one output, and twenty hidden layers

The activation function $f(u_i)$ used is the hyperbolic tangent function:

$$f(u_i) = \tanh(u_i) = \frac{1 + e^{-u_i}}{1 - e^{-u_i}} \quad (4)$$

where u_i refers to the net inside activity level of the i -th neuron in the hidden layer. The net inside activity level u_i is defined as :

$$u_i = \sum_{j=1}^{n=5} \sum_{i=1}^{n=20} W_{ij} a_j + b1_i \quad (5)$$

where W_{ij} refers to corresponding weights and biases $b1_i$ based on the inputs a_j . With respect to the five inputs, Eq. (5) can be written as:

$$u_i = W_{i,1} \cdot \text{current} + W_{i,2} \cdot \text{windstrength} + W_{i,3} \cdot \text{vesselspeed} + W_{i,4} \cdot \text{winddirection} + W_{i,5} \cdot \text{avg.draft} + b1_i \quad (6)$$

The outputs from the hidden layer are then used as inputs to the output layer. This is passed through the activation function $f(k_i)$:

$$f(k_i) = \tanh(k_i) = \frac{1 + e^{-k_i}}{1 - e^{-k_i}} \quad (7)$$

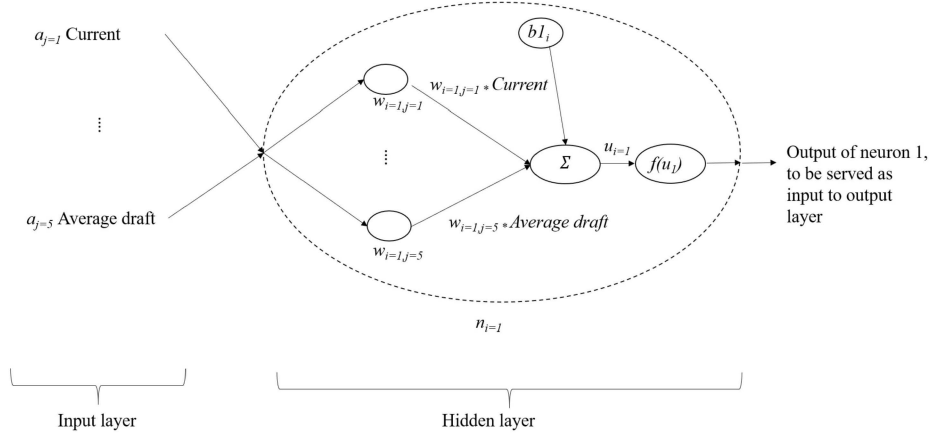


Figure 4: Working mechanism inside a single neuron. This neuron refers to hidden layer 1.

where k_i refers to the net output activity level of the i -th neuron in the hidden layer. The net output activity indicator k_i is:

$$\begin{aligned}
 k_i &= \sum_{i=1}^{n=20} f(u_i) \cdot lw_i + b2 \\
 &= \sum_{i=1}^{n=20} \frac{1 + e^{-u_i}}{1 - e^{-u_i}} \cdot lw_i + b2
 \end{aligned} \tag{8}$$

where n refers to the number of hidden layers. Each hidden layer node n_i has its own weights (identified as lw_i). The bias at the output level is defined as $b2$. In this paper, 20 hidden layers have been utilised after investigation that any increase in the number of hidden layers does not improve the R^2 value. The training and validation sets of the data are split in 70-30 % ratio.

The model yielded an overall R^2 value of 0.8800 (see Figure 6). The training set obtained a R^2 value of 0.9048, while the validation and testing set had a value 0.8501 and 0.8411 respectively.

The weights and biases in the ANN are summarised below (see Table 6):

4. Validation and benchmarking

The model is validated through two ways. The first is by looking at the goodness-of-fit for the model. The second is by comparing the results to the situations which may relate to the overall ship resistance and hence

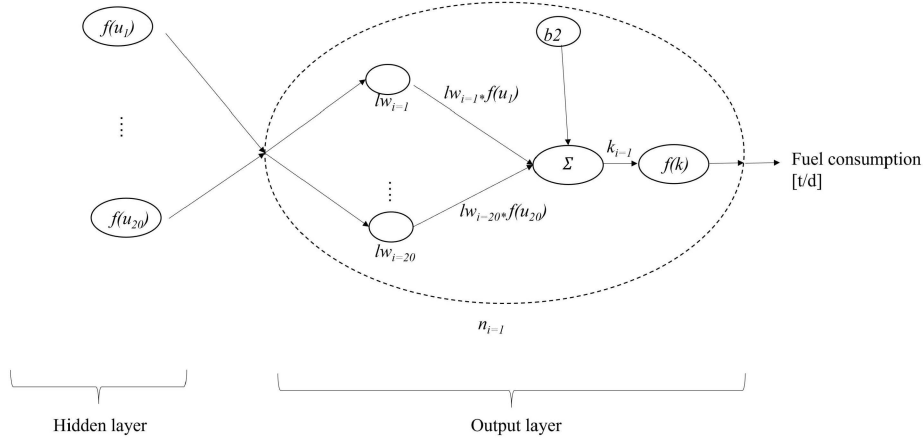


Figure 5: Working mechanism inside a single neuron at the output layer.

the derived fuel-speed curve. The goodness of fit ($R^2 = 0.884$) values from this analysis are considered satisfactory. Similar applications of ANN to different ship operations demonstrate that 'acceptable' R^2 values are 0.744 to 0.834 for fuel prediction for oil tankers [19]. In addition to using R^2 values as a goodness-of-fit indication, the results corresponding to the physical phenomenon is also used to assess the model performance.

The simulated data (see Figure 7 and 8) demonstrates that the ANN model can derive results according to the steepest propeller curve (Profile 1) and the most gentle propeller curve (Profile 2) in accordance to the different operating conditions stemming from the sea-state and thus the overall resistance to the vessel. In Figure 7, Leg 1: Profile 1 refers the sea state conditions that suggests the highest resistance the ship might face, such as high current against the vessel, head wind of strength of Beaufort scale 7 (which is considered as high wind, near gale strength) and at an average draft of 14 m. The histograms (see Figure 9) show that the current, wind strength and associated draft from cargo load experienced is in the upper end of the distribution of sea state conditions of the vessel experience. Leg 1: Profile 2, which reflects a much gentler propeller curve indicates that the resistance a ship is experiencing is much lesser. Current is significantly lesser at almost zero. While the ship experiences headwind, it is a Beaufort strength 5, it is 2 states lower and is considered a 'fresh breeze' as compared to Leg 1: Profile 1. In addition, the average draft is at 13 m, implying lesser cargo load. Leg 1: Profile 3 has conditions in between that of Leg 1: Profile 1 and 2. The current against the vessel is lesser at -0.8 kn, and the average

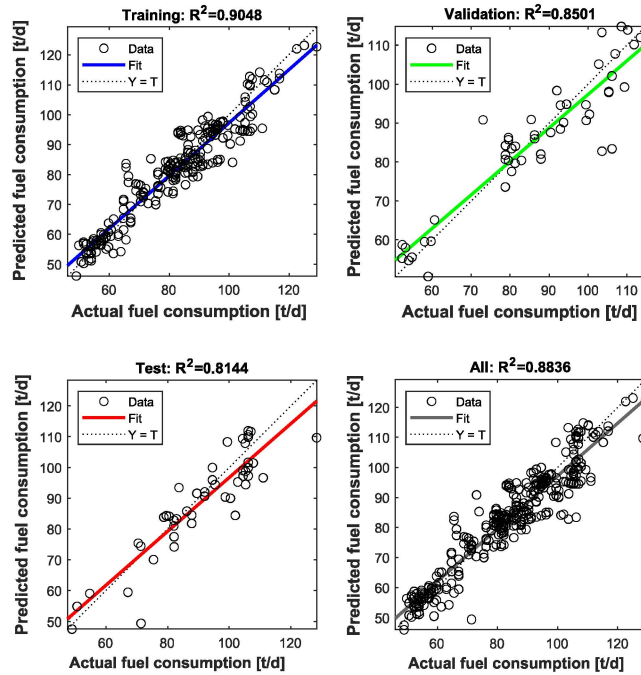


Figure 6: Plot of the actual and predicted fuel consumption in Leg 1 within a channel. The predictions are broken down into output from training, validation, test data sets and overall results.

draft is of a lower value than Leg 1: Profile 1. Wind conditions remain at headwind and at Beaufort strength 7, similar to Leg 1: Profile 1. Overall Leg 1: Profile 1 reflects a scenario where the sea-state conditions suggest that the ship would experience high resistance, and Leg 1: Profile 2 reflects a scenario where the sea-state conditions is more conducive for a lower ship resistance. Leg 1: Profile 3 refers to a scenario in between them. A similar plot to Figure 7 except with fuel-speed power curves plotted from the simulated results demonstrate that the power coefficients are in the range of 2.21 to 3.13, which agree with literature review of container ships by Wang et al [8] and Adland et al [5].

It can be observed that the first NN presented reflects the environment within rather closed waters as there is another island that simulates travelling within a channel.

An analysis of another leg of the vessel journey is based on travelling

Table 2: Weights and biases in the ANN. See Eqs (6) & (8)

n	W_{i1}	W_{i2}	W_{i3}	W_{i4}	W_{i5}	l_w	$b1$	$b2$
1	0.3182	-0.1767	-0.9280	3.959	0.6833	0.156	-3.603	0.0448
2	1.0129	0.8684	-1.7210	3.3834	-2.0642	-0.3224	5.0481	
3	-0.7675	1.5010	1.0198	0.6436	-1.8524	0.6949	-0.5875	
4	-4.6135	-1.7680	-4.3690	-1.5216	3.1281	0.2176	3.0596	
5	-1.0453	-3.0860	-2.4904	-1.5757	3.5233	-0.1618	3.2163	
6	-0.5871	-0.3435	-5.6738	3.3350	1.0151	-0.1683	3.0262	
7	-0.0034	-0.7860	2.6684	-0.8905	1.1342	0.2061	2.9490	
8	-2.2038	-0.6202	0.4561	2.6423	-0.2203	-1.2714	-1.1539	
9	0.3652	1.2574	-2.5649	-1.0541	0.9890	-0.1365	-1.6418	
10	-3.3971	0.3049	0.7089	-1.1972	0.2492	-0.1810	0.2392	
11	-0.7620	-2.8466	-0.5012	0.5669	0.3166	0.3740	-1.9342	
12	-3.8127	-1.4858	-1.1629	1.3434	0.9851	0.1149	0.5971	
13	-1.7807	-0.2802	0.4893	1.7727	0.0218	1.7326	-0.7216	
14	1.6415	-0.8688	-4.6067	-1.0624	-2.6141	0.2545	2.1147	
15	2.6458	-2.2624	0.3082	-2.4584	-2.9388	-0.1428	4.3786	
16	2.0198	0.1407	-0.3368	1.1250	4.7158	0.4616	2.8408	
17	3.6052	1.2295	-0.2614	0.8858	-1.8925	-0.0457	2.6464	
18	-1.8330	-2.8262	1.6702	-1.9683	1.6982	-0.2329	-3.6153	
19	0.9197	-4.9122	-3.5518	0.2605	3.3848	0.2245	1.7562	
20	0.2493	2.6183	0.4218	-2.2200	-4.5869	0.1746	-1.9334	

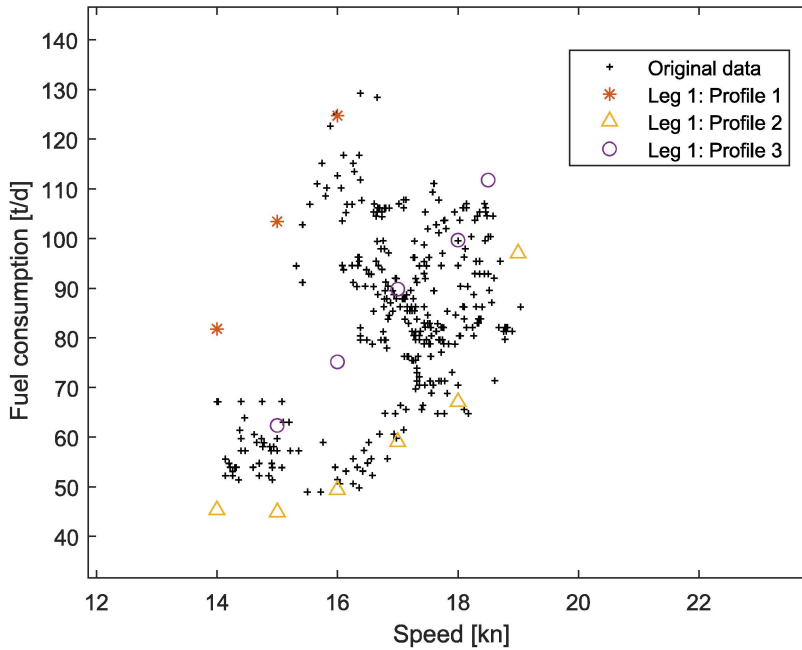


Figure 7: A plot of the original data demarcated in black and three fuel-speed curves simulated from three differing profile. Profile 1 suggests sea-state conditions which will results in higher ship resistance, while Profile 2 suggest sea-state conditions resulting in lower ship resistance. Profile 3 suggests sea state conditions that are in between that of Profile 1 and 2.

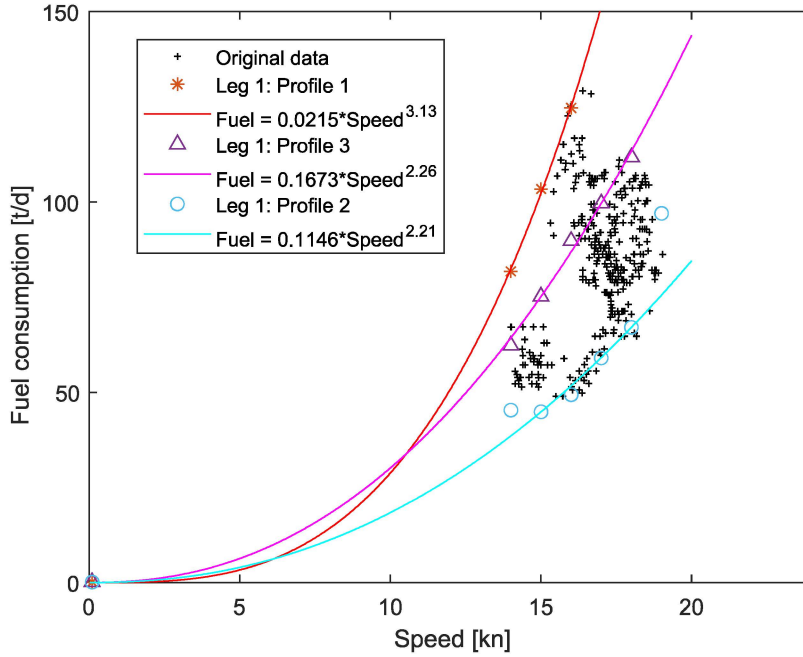


Figure 8: A similar plot to Figure 7 except with fuel-speed power curves plotted from the simulated results. The power coefficients are in the range of 2.21 to 3.13, which agree with literature review of container ships by Wang et al [8] and Adland et al [5].

through open water in the Indian Ocean. The plot of the actual and predicted fuel consumption using the ANN model is demonstrated in Figure 10. The overall R^2 value at 0.8675 is comparable to the ANN model for Leg 1 of the journey. The KDE plot (Figure 11), fuel-speed plot (Figure 12, as clustered and colour coded according to the KDE) and the description of the sea-state for the most frequently occurring fuel-speed profile is found in Figure 13.

The simulated results (Figure 14) demonstrate that the ANN model is capable of deriving different Fuel-Speed curves according to the resistance that the ship faces not only in close conditions (such as through a channel) but also in open water conditions. The difference in resistance is largely due to the sea-state conditions.

It can be observed that the fuel-speed data in Leg 2 of the journey has a largely horizontal profile which may appear odd as this implies the fuel consumed does not change even as vessel speed changes from 14 kn to 19

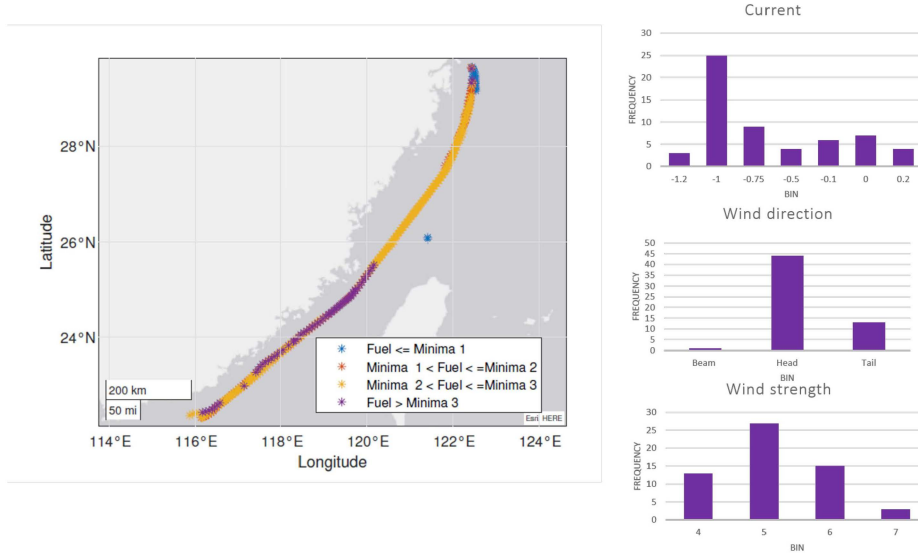


Figure 9: A geographical plot of the original data. The histograms in the right of the figure refer to the sea-state conditions of the journey demarcated in purple within a channel. The purple plots in the geographical plot indicate where the fuel consumption is the highest. The minimas refer to the KDE probability density plot in Figure 1.

kn. One explanation for this observation is that the sea-state conditions actually reduce the ship resistance such that the fuel consumed for the same or greater speed is lesser, such as wind and current pushing a vessel along in the direction of travel, as opposed to working against wind and current along the journey.

Leg 2: Profile 1 describes a scenario where current and wind is working against the vessel such that the overall ship resistance is increased. Current is at -0.77 kn, with headwind at wind strength at Beaufort scale 5 (Fresh breeze). Leg 2: Profile 2 differs from Profile 1 in terms of current only, where current is positive, i.e. pushing the vessel in its intended direction of travel at 0.7 kn. Leg 2: Profile 3 describes the sea-state that is in between Profile 1 and 2 by having current assisting the vessel, but at a lower magnitude than Profile 2, and lesser headwind at Beaufort scale 3 (Gentle breeze).

It is also interesting to note that at higher vessel speeds such as at 19 kn, when the sea-state is such that it reduces the overall resistance faced by a vessel, the ANN model can capture the observation that the fuel consumption for the addition 1 kn at 19 kn of vessel speed is only a little bit more than at 18 kn.

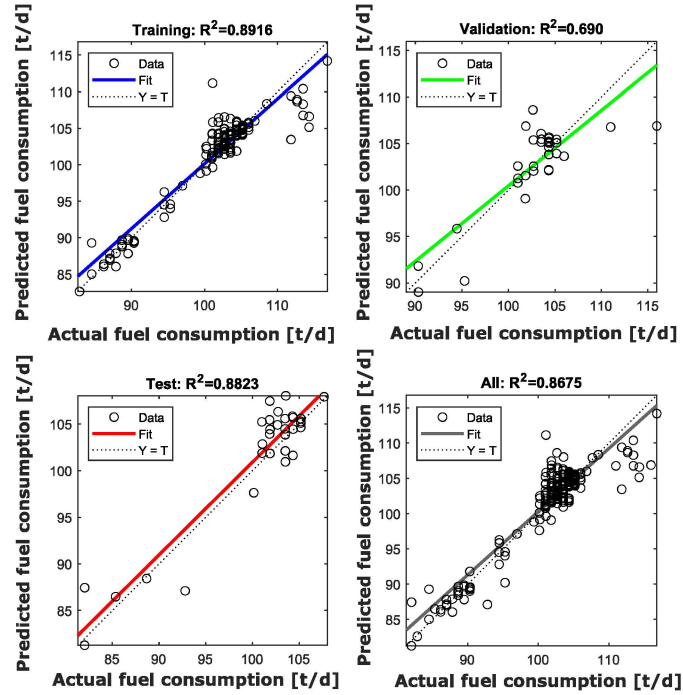


Figure 10: Plot of the actual and predicted fuel consumption in Leg 2, a journey in the Indian Ocean. The predictions are broken down into output from training, validation, test data sets and overall results.

5. Improving energy efficiency in ships

It is generally understood that most research on optimising vessel operations attempt to predict or have snapshots, as accurately as possible, the ship resistance. The summary of the proposed method in this paper is attempting to provide snapshots of the ship resistance under different sea-state conditions. One novelty of this paper is the derivation of fuel-speed curves from actual data. These fuel-speed curves capture elements that the design fuel-speed curves do not.

Adland et al [5] investigated and demonstrated that the elasticity of fuel consumption of oil tankers varies across speeds and sea-states. The article suggests that the 'cubic law' is only true near the design speed of vessels and conditions set out in the speed trial analysis. In the same way that engine load diagrams have different curves for recommended operations or heavy

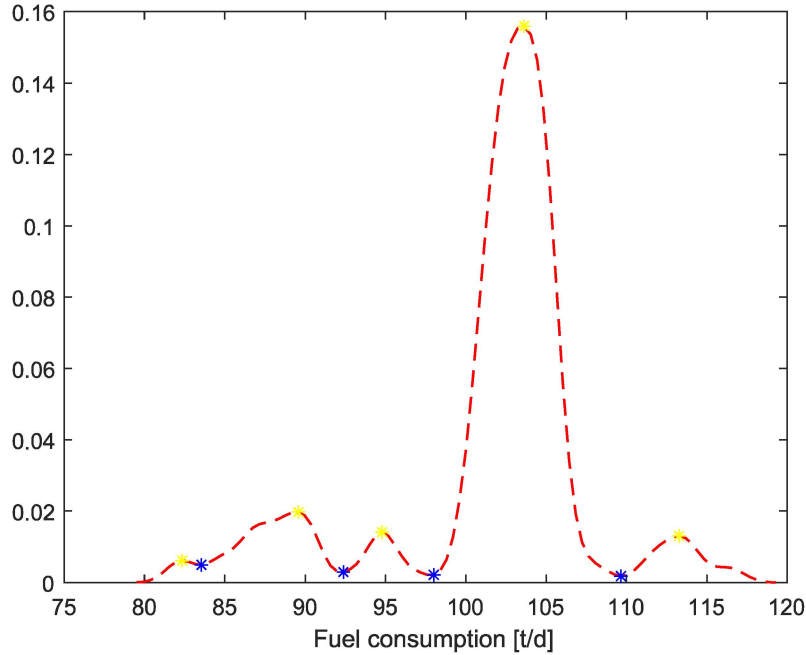


Figure 11: A kernel density estimate constructed using the data of fuel consumption[t/d] for a vessel journey in the Indian Ocean.

operations, the derived fuel-speed curves from the telemetry data indicated that within a vessel leg where the cargo remains constant, the different sea-states affect the fuel consumption of the vessel.

For a given voyage, the fuel consumption is not just affected by the speed of the vessel. Figure 7 shows that while travelling at 17 kn, the vessel may consume between 85 t/d to 115 t/d due to the sea-state that affects the overall ship resistance. If considering the impact of slow-steaming on CO_2 emissions simply based on design propeller curves, there could be an overestimation in the reduction of CO_2 emissions. Vessel operations are dynamic and thus the optimal speed changes according to the sea-state. With the provision of parameter information on the average draft, the wind strength and direction and impact of current, the optimal speed according to the ideal fuel to be consumed can then be estimated. Or, in the case of cargo vessels which travel mostly to meet a delivery schedule (i.e. there is priority of reaching destination over emissions control or fuel economy), a more accurate fuel consumption pattern can be derived, from which a more

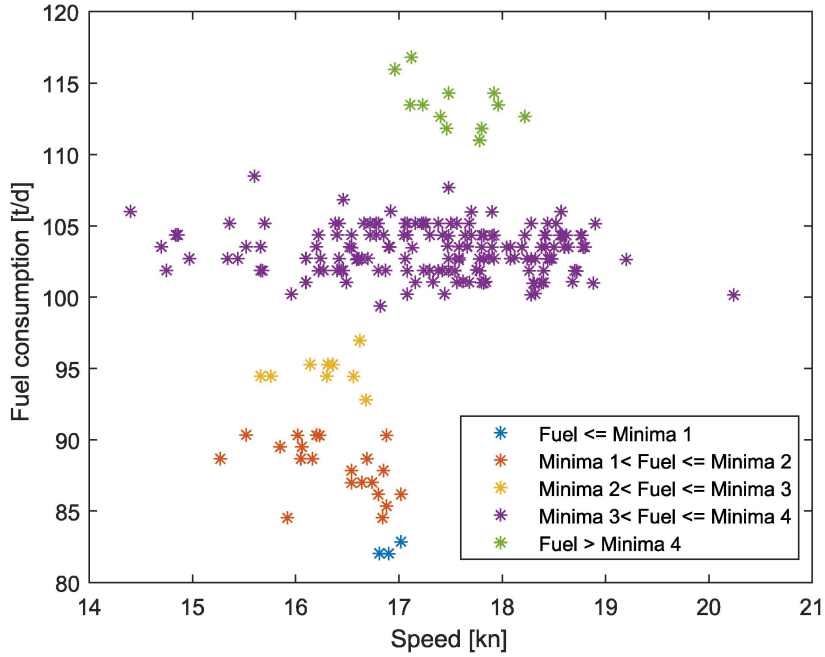


Figure 12: Fuel consumption for vessel journey between two ports in Leg 2 of the journey. The clustering of data (colour coded) is done so with respect to the KDE of Figure 11). The 2 clusters plotted geographically also could indicate different sea states that resulted in difference in fuel consumptions. This can be cross referred to Figure 13.

accurate emissions analysis can be undertaken. The impact of maritime policy such as slow-steaming or changing the constituents of marine fuel can then be more accurately assessed.

6. Conclusion

In this paper, a systematic methodology for deriving vessel and journey specific fuel-speed curve from ship telemetry data has been carried out. Kernel densities estimation is used to categorise operational profiles, and then an ANN is used to derive the relationship between fuel consumed and vessel speed, vessel average draft and sea-state conditions. The method demonstrated that it was able to deduce fuel-speed curves in close-sea conditions such as within a channel, and open-sea conditions in the Indian Ocean. In both conditions, the fuel-speed curves varied according the sea-state thus

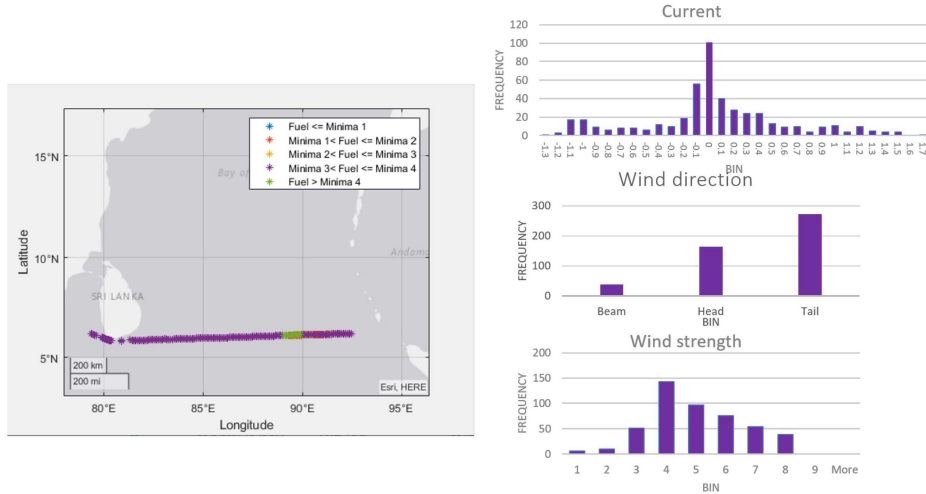


Figure 13: A geographical plot of the original data. The histograms in the right of the figure refer to the sea-state conditions of the journey demarcated in purple within a channel. The purple plots in the geographical plot indicate where the fuel consumption is the highest. The minimas refer to the KDE probability density plot in Figure 1.

highlighting that the different working loads experienced by the vessel can be captured by the model. In addition, the model is validated by comparable R^2 values with other statistical/machine learning methods, as well as by analysis of the physical phenomena (i.e. based on domain knowledge) of the conditions that affect the ship resistance. In summary, the method allowed a more accurate prediction of fuel consumption, and a vessel specific understanding of what is considered optimal speed. It is thus inferred that the method on analysing telemetry data demonstrates consistent results, and benefitting the industry with improved maritime practices or streamlined vessel operation. This encourages better data collection practices in the industry which will become a valuable big data push for the maritime industry.

7. Future work

With the IMO requirement on the data monitoring on fuel consumption for vessels greater than 5000 tonnes, the method can be extended to provide greater insights to engine performance. Tillig et al [20] highlighted that maximising fuel efficiency of existing ships is crucial but the sole solution of optimizing the maintenance and operation of existing ships will not aid

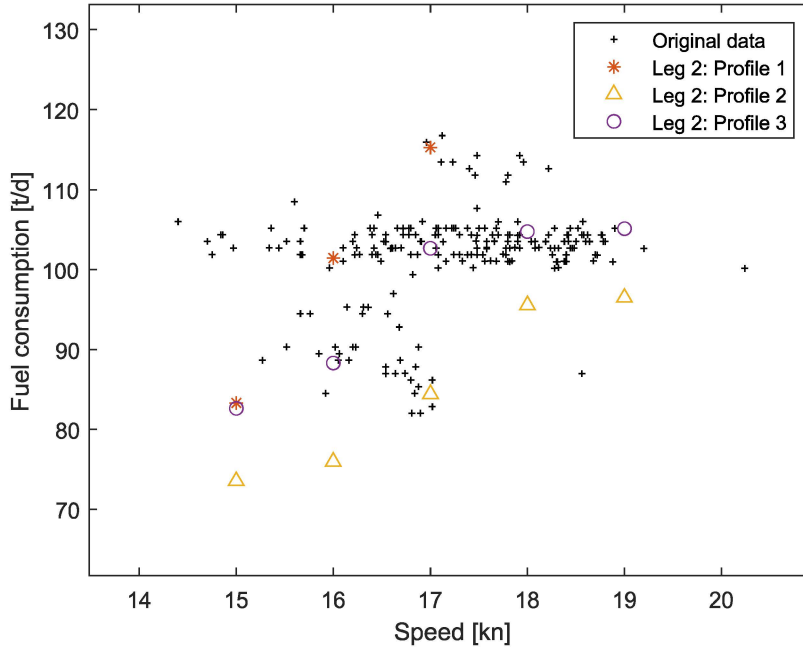


Figure 14: A plot of the original data (Leg 2: Indian Ocean) demarcated in black and 3 fuel-speed curves simulated from 3 differing profile. Profile 1 suggests sea-state conditions which will results in higher ship resistance, while Profile 2 suggest sea-state conditions resulting in lower ship resistance. Profile 3 suggests sea state conditions that are in between that of Profile 1 and 2.

the shipping industry in achieving the IMO goals. To cut the emissions of shipping by the targeted 50%, drastic measures must be taken in the design, operation and propulsion of ships. For this purpose, a ship energy systems model must be capable of predicting the performance of generic ships prior to the actual design phase or retrofitting of existing ships with alternative propulsions systems. This method of deriving the fuel-speed curves from kernel probability densities as outlined in this paper is actually a simplified method by Tsitsilonis et al [16]. Tsitsilonis et al [16] attempts to classify the 2 coefficients of the propeller curve by utilising KDEs of the engine rotational speed to determine the most frequently occurring operational profile. Within the operation profile of the engine rotational speed, the corresponding engine characteristics such as the air filter pressure, the compressor outlet temperature etc to conduct energy and exergy analysis.

1
2
3
4
5
6
7
8
9
10 The output of such analysis can give holistic direction to the problematic
11 areas engine operational point that corresponds to low efficiency, in which
12 such analysis is sensitive to a specific ship (its hull design, propeller design
13 etc) and sea-state conditions.
14

15 **Acknowledgement**

16
17 The authors would like to acknowledge the support of the Ministry of Ed-
18 ucation of Singapore (MOE-SIT Ignition Grant R-MOE-E103-F010). The
19 authors are grateful for the extensive support and knowledge sharing from
20 Mr. Thong Sew Kait in the undertaking of this work. His insights and
21 thought-provoking comments help shape the outcome of this paper.
22
23
24

25 **References**

26
27
28
29
30
31
32
33
34
35
36
37
38
39
40
41
42
43
44
45
46
47
48
49
50
51
52
53
54
55
56
57
58
59
60
61
62
63
64
65

- 1
2
3
4
5
6
7
8
9
10 [1] M. Stopford, *Maritime economics*, 3rd Edition, Vol. 47, Taylor and
11 Francis, New York, 2010.
- 12 [2] D. Ronen, The effect of oil price on containership speed and fleet size,
13 *Journal of the Operational Research Society* 62 (1) (2011) 211–216.
14 doi:10.1057/jors.2009.169.
15 URL <https://doi.org/10.1057/jors.2009.169>
- 16 [3] International Maritime Organisation, *Reducing greenhouse gas emis-*
17 *sions from ships* (2018).
18 URL [https://www.imo.org/en/MediaCentre/HotTopics/Pages/](https://www.imo.org/en/MediaCentre/HotTopics/Pages/Reducing-greenhouse-gas-emissions-from-ships.aspx)
19 [Reducing-greenhouse-gas-emissions-from-ships.aspx](https://www.imo.org/en/MediaCentre/HotTopics/Pages/Reducing-greenhouse-gas-emissions-from-ships.aspx)
- 20 [4] N. Bialystocki, D. Konovessis, On the estimation of ship’s fuel
21 consumption and speed curve: A statistical approach, *Journal of Ocean Engineering and Science* 1 (2) (2016) 157–166.
22 doi:10.1016/j.joes.2016.02.001.
23 URL <http://dx.doi.org/10.1016/j.joes.2016.02.001>
- 24 [5] R. Adland, P. Cariou, F. C. Wolff, Optimal ship speed and the cubic
25 law revisited: Empirical evidence from an oil tanker fleet, *Transportation Research Part E: Logistics and Transportation Review* 140 (May)
26 (2020) 101972. doi:10.1016/j.tre.2020.101972.
27 URL <https://doi.org/10.1016/j.tre.2020.101972>
- 28 [6] E. F. Magirou, H. N. Psaraftis, T. Bouritas, The economic speed of an
29 oceangoing vessel in a dynamic setting, *Transportation Research Part B: Methodological* 76 (2015) 48–67. doi:10.1016/j.trb.2015.03.001.
30 URL <http://dx.doi.org/10.1016/j.trb.2015.03.001>
- 31 [7] Z. Yao, S. H. Ng, L. H. Lee, A study on bunker fuel management for
32 the shipping liner services, *Computers and Operations Research* 39 (5)
33 (2012) 1160–1172. doi:10.1016/j.cor.2011.07.012.
34 URL <http://dx.doi.org/10.1016/j.cor.2011.07.012>
- 35 [8] S. Wang, S. Gao, T. Tan, W. Yang, Bunker fuel cost and freight revenue
36 optimization for a single liner shipping service, *Computers and Operations Research* 111 (2019) 67–83. doi:10.1016/j.cor.2019.06.003.
37 URL <https://doi.org/10.1016/j.cor.2019.06.003>
- 38 [9] Q. Meng, Y. Du, Y. Wang, Shipping log data based container ship fuel
39 efficiency modeling, *Transportation Research Part B: Methodological*
40 83 (2016) 207–229. doi:10.1016/j.trb.2015.11.007.
41
42
43
44
45
46
47
48
49
50
51
52
53
54
55
56
57
58
59
60
61
62
63
64
65

- 1
2
3
4
5
6
7
8
9
10 [10] M. W. Ng, Vessel speed optimisation in container shipping: A new
11 look, *Journal of the Operational Research Society* 70 (4) (2019) 541–
12 547. doi:10.1080/01605682.2018.1447253.
13 URL <http://doi.org/10.1080/01605682.2018.1447253>
14
- 15 [11] H. Lindstad, B. E. Asbjørnslett, E. Jullumstrø, Assessment of profit,
16 cost and emissions by varying speed as a function of sea conditions
17 and freight market, *Transportation Research Part D: Transport and*
18 *Environment* 19 (2013) 5–12. doi:10.1016/j.trd.2012.11.001.
19 URL <http://dx.doi.org/10.1016/j.trd.2012.11.001>
20
- 21 [12] L. Leifsson, S. Hildur, S. Sigurasson, A. Vesteinsson, Simula-
22 tion Modelling Practice and Theory Grey-box modeling of an
23 ocean vessel for operational optimization 16 (2008) 923–932.
24 doi:10.1016/j.simpat.2008.03.006.
25
- 26 [13] A. Coraddu, L. Oneto, F. Baldi, D. Anguita, Vessels fuel consump-
27 tion: A data analytics perspective to sustainability, Vol. 358, 2018.
28 doi:10.1007/978-3-319-62359-7₂.
29
- 30 [14] M. M. Abdel Naby, H. W. Leheta, A. A. Banawan, A. H. Elhewy, Investi-
31 gation of various artificial neural networks techniques for the prediction of
32 inland water units’ resistance, *Ships and Offshore Structures* 3 (3) (2008)
33 247–254. doi:10.1080/17445300802048364.
34
- 35 [15] S. Wang, Q. Meng, Sailing speed optimization for container ships in a liner
36 shipping network, *Transportation Research Part E: Logistics and Trans-
37 portation Review* 48 (3) (2012) 701–714. doi:10.1016/j.tre.2011.12.003.
38 URL <http://dx.doi.org/10.1016/j.tre.2011.12.003>
39
- 40 [16] K. M. Tsitsilonis, G. Theotokatos, A novel systematic methodology for
41 ship propulsion engines energy management, *Journal of Cleaner Production*
42 204 (August) (2018) 212–236. doi:10.1016/j.jclepro.2018.08.154.
43
- 44 [17] P. Andersen, A. S. Borrod, H. Blanchot, Evaluation of the service perfor-
45 mance of ships, in: *Marine Technology and SNAME News*, Vol. 42, 2005,
46 pp. 177–183. doi:10.5957/mt1.2005.42.4.177.
47 URL <https://doi.org/10.5957/mt1.2005.42.4.177>
48
- 49 [18] D. G. M. Watson, *Practical Ship Design, Volume 1*, Vol. 1, 1998.
50 URL <http://www.sciencedirect.com/>
51
52
53
54
55
56
57
58
59
60
61
62
63
64
65

1
2
3
4
5
6
7
8
9
10
11
12
13
14
15
16
17
18
19
20
21
22
23
24
25
26
27
28
29
30
31
32
33
34
35
36
37
38
39
40
41
42
43
44
45
46
47
48
49
50
51
52
53
54
55
56
57
58
59
60
61
62
63
64
65

[19] E. Bal Beikçi, O. Arslan, O. Turan, A. I. Ölçer, An artificial neural network based decision support system for energy efficient ship operations, *Computers and Operations Research* 66 (January 2013) (2016) 393–401. doi:10.1016/j.cor.2015.04.004.

[20] F. Tillig, J. W. Ringsberg, H. N. Psaraftis, T. Zis, Reduced environmental impact of marine transport through speed reduction and wind assisted propulsion, *Transportation Research Part D: Transport and Environment* 83 (2020) 102380. doi:10.1016/j.trd.2020.102380.
URL <https://doi.org/10.1016/j.trd.2020.102380>